International Journal of Chemical, Material and Environmental Research 2016, 3 (2): 20-28

Research article

IJCMER
www.ijcmer.org

INTERNATIONAL JOURNAL OF CHEMICAL, MATERIAL AND ENVIRONMENTAL RESEARCH

An International Open Free Access, Peer Reviewed Research Journal

ISSN 2410-5945
2016, Vol. 3, No. 2:
pg. 20-28

Nanostructured TiO_2 Obtained by Electrolysis and its Application in the Remediation of Water Polluted with Paracetamol

Roberto Fernández-Acosta[1, 2], Ernesto Peláez-Abellán[3], José R. Correa[3], Ulises Jáuregui-Haza [1, *]

[1] Instituto Superior de Tecnologías y Ciencias Aplicadas. Avenida Salvador Allende, esquina Luaces, Quinta de los Molinos, La Habana, Cuba
[2] Instituto de Farmacia y Alimentos, Universidad de La Habana. Calle 222, # 2317, La Coronela, La Lisa, La Habana, Cuba
[3]Facultad de Química, Universidad de La Habana. Calle Zapata, e/ G y Carlitos Aguirre, Plaza de la Revolución, La Habana, Cuba

(Received: April 25, 2016; Accepted: June 09, 2016)

Abstract

The heterogeneous photocatalysis constitutes an efficient alternative for the treatment of wastewaters polluted with toxic and recalcitrant substances . In this work, the characterization of TiO_2 nanomaterial obtained by an electrolytic procedure, and its evaluation to degrade paracetamol in aqueous solution are presented. The characterization with X-rays diffraction, Fourier transform infrared spectroscopy and energy dispersive X-ray spectroscopy, evidenced the obtaining of the material. The particle size, determined by transmission electron microscopy, was 9.3 nm ± 2.7 nm and the surface area was 115,4 m^2/g according to the Brunauer-Emmett-Teller isotherm. The resulting optical band gap of the sample, determined by diffuse reflectance spectroscopy, was 3.15 eV (393 nm). The obtained nanoparticles were tested in the photodecomposition of paracetamol. Approximately 60% of pollutant was degraded with sun light, and 76% with artificial UV light.

Keywords: Paracetamol, heterogeneous photocatalysis, TiO_2 nanomaterial

1. Introduction

The social and economic development goes together with the increase of the industrial activity. Consequently, a huge amount of substances enter into the water cycle through different routes [1-4]. Among these emergent pollutants it can be found the persistent organic pollutants (POPs), which enter the surface waters mainly through the untreated residual waters, and through the residual waters coming from conventional waste water treatment stations, which are not designed to treat these recalcitrant substances [2, 5]. The drugs are particular POPs, distinguished for its high consumption at world level, which up to 100 000 t/year corresponding to an annual global consumption of 15 g/per capita [3, 4]. The presence of drugs and their metabolites in waters causes different health problems as bacterial resistance and multi-resistance to antibiotics, genotoxicity and mutagenicity, endocrine disruption, cancer and miscarriages in pregnant women [2-4, 6-11]. The advanced oxidation processes (AOPs) are one of the most promising alternatives for water treatment. AOPs have been defined as ambient temperature and pressure processes that involve the generation of highly reactive intermediates, particularly the hydroxyl radicals ($OH^{\cdot}$), which react rapidly and indiscriminately with most organic compounds [12-16]. Semiconductor photocatalysis is one of the most promising AOPs for the degradation of aquatic pollutants [7]. TiO_2 is one of the most use-

* Corresponding author:
ulises.jauregui@infomed.sld.cu
Published online at www.ijcmer.org

ful photocatalyst because of its high photostability and photoreactivity, nontoxicity, low cost, and chemical and biological inertness [17]. On the other hand, the use of artificial UV light ($\lambda \leq 387$ nm) and the decrease of quantum yield by electron-hole recombination, are some disadvantages that require being overcome for the best use of this material [14].

The aim of this work is to characterize a TiO_2 nanomaterial, obtained by electrolytic process, and to evaluate its ability to degrade paracetamol in aqueous solution. Paracetamol was selected as model pollutant because it is one of most popular drugs at world level. In addition, from 58% to 68% of paracetamol is excreted unmetabolized after therapeutic use [18]. Additionally, some metabolites of this drug are hepatotoxic, as the imine-N-acetyl-p-benzoquinone. When the drug is treated by some conventional treatment, as chlorination, toxic byproducts, such as genotoxic and mutagenic 1,4-benzoquinone imine and N-acetyl-p-benzoquinone; are produced [3, 4, 19]. These reasons, together with paracetamol's solubility in water (14 g/L), let us consider this drug as a pollutant of interest.

2. Materials and Methods

2.1. Chemicals

Paracetamol (99%) from Sigma-Aldrich; H_2O_2 (30%) and H_3PO_4 (85%) from Fluka; acetonitrile from Scharlau-Chemie; sodium dodecyl sulfate (99%), Na_2SO_3, ethanol, and KBr, from Merck; NaCl (99%) from Riedel-de Haen AG and KI from BDH Laboratory were used.

2.2. Synthesis of TiO_2 Nanomaterial

The TiO_2 was synthesized by a novel electrolytic process according to patent 120711 CU [20]. The electrolysis was performed by using an anode of Ti obtained from scrap or waste originated during replacement of different parts of the factory of nickel "Ernesto Che Guevara" in Moa, Holguín, Cuba. A circular stainless steel plate was used as cathode. The chemical composition of both electrodes are shown in Tables 1 and 2 [21].

Table 1. Chemical Composition of the Ti Alloy Used as Anode for Obtaining TiO_2

Elements	Si	Fe	Cr	Ni	Ti
Chemical composition (%)	4.5	5.2	6.0	6.6	77.7

Table 2. Chemical Composition of the Stainless Steel Plate Used as Cathode for Obtaining TiO_2

Elements	Si	Mn	Ni	Cu	Cr	V
Chemical composition (%)	0.287	0.483	0.165	0.098	18.87	0.11

The electrolysis was carried out in hydro-alcoholic solution saturated in NaCl, in the presence of sodium dodecyl sulfate solution using a 4–8 mA/cm^2 range of current density, during 48 h. The obtained product was left to stand for 24 h. Subsequently, it was washed with distilled water in order to reach established technological parameters. Then, the colloidal dispersion was concentrated, and a portion was dried in an oven at 120^0C, until constant weight, in order to obtain TiO_2 nanopowder.

2.3. Characterization of TiO_2 Nanoparticles

2.3.1. X-ray Diffraction (XRD)

The XRD analysis was performed at room temperature on the dried nanopowder using a Rigaku Rotaflex Ru-200 B diffractometer. The crystallite size was calculated by Scherrer equation.

2.3.2. Fourier Transform Infrared Spectroscopy (FT-IR)

Spectra were recorded in solid phase, with KBr pellets, using a Perkin Elmer Spectrum One spectrophotometer in the 4000 cm^{-1}-400 cm^{-1} range.

2.3.3. Diffuse Reflectance Spectroscopy (DRS)

Optical spectra of the samples, followed by their Eg values, were acquired on a Shimadzu UV 3100 spectrometer, using $BaSO_4$ as reference. The Kubelka–Munk function was applied with the aim of converting the diffuse reflectance into the absorption coefficient α (Equation 1).

$$\alpha \approx \frac{K}{S} = \frac{(1-R_\infty)^2}{2R_\infty} \equiv F(R_\infty) \quad (1)$$

where *K* and *S* are the absorption and scattering coefficients and the reflectance R_∞ is equal to $R_{sample}/R_{reference}$ [22].

The *Eg* of the sample was calculated using the Tauc plot (Equation 2).

$$(\alpha \, h\nu)^\gamma = A(h\nu - E_g) \quad (2)$$

where *A* is a material constant, *h* is the Planck's constant, *v* is the frequency of the light, *Eg* is the energy band gap of the allowed transitions, and γ is the power coefficient characteristic for each type of transition. For nanoscale semiconductor materials, the value of γ is accepted to be equal to 0.5, because the transition is assumed to be indirectly allowed [23]. Therefore, it is possible to determine the energy band gap of the semiconductor material from the x-axis (α = 0), by plotting $[F(R_\infty)h\nu]^{0.5}$ against hν, and adjusting to a straight line the points of the function after the turning point.

2.3.4. Transmission Electron Microscopy (TEM) and Energy Dispersive X-ray Spectroscopy (EDS)

TEM analysis was performed using a Philips CM200 FEG microscope equipped with an EDS detector. Samples for TEM observations were prepared by dispersing the nanoparticles (NPs) in ethanol and evaporating the suspension drops on carbon-coated copper grids. EDS measurements were performed in the same experiment. To count and to measure the NPs, ImageJ software was used.

2.3.5. BET Isotherm

The surface area of the prepared sample was evaluated by the Brunauer–Emmett–Teller (BET) method (Micrometrics ASAP-2000 equipment) using N_2.

2.4. Evaluation of Photocatalytic Activity (PCA)

The PCA of the prepared TiO_2 was evaluated under both UV-light and visible-light irradiation by determining the degradation of paracetamol in aqueous solution. The tests were performed during 90 minutes, at room temperature, pH equal to 5.5, and H_2O_2 concentration of 41.7 mmol/L. A cylindrical photocatalytic reactor (100 mm inner diameter) containing 50 mL of aqueous solution of paracetamol (initial concentration of 0.1 g/L) was used. The concentration of the photocatalyst in the slurry was 0.5 g/L. The UV-light source was a mercury-vapor lamp (254 nm, Philips TUV 11 W), placed at the surface of reactor (unidirectional irradiation). At the end of reaction, the catalyst was separated by filtration through nylon filters of 0.2 µm of pore diameter, and the paracetamol concentration in the liquid phase was then determined by high performance liquid chromatography (HPLC). A SHIMADZU chromatograph (Prominensce High Pressure) with a diode array detector DAD UV/Vis SHIMADZU SPD-M20A, with a Shim pack CLC C8 (M) type column (length of 250 mm,inner diameter of 4.6 mm, filled with spherical silica of 5 µm) was used. The flow of the mobile phase was 1mL/min and the process temperature was 40^0C. The injection volume and wavelength were 100 µL and 254 nm, respectively. Mobile phase was a 90:10 mixture (V/V) of water acidified with phosphoric acid (pH = 3) and acetonitrile. The extent of paracetamol photocatalytic degradation (%D) was evaluated by Equation 3.

$$\%D = \frac{c_0 - c}{c_0} 100 \quad (3)$$

where c_0 is the initial paracetamol concentration and c is the concentration after the irradiation time.

When H_2O_2 was used, the samples were treated with quenching solution of NaOH, Na_2SO_3 and KI, in order to stop the oxidation process [24]. The extent of paracetamol photocatalytic mineralization (%M) was evaluated by the Equation 4. The total organic carbon (TOC) concentration was determined by a Shimadzu TOC-VCSN analyser.

$$\%M = \frac{c_0(TOC) - c(TOC)}{c_0(TOC)} 100 \quad (4)$$

where $c_0(TOC)$ and $c(TOC)$ are the initial and final concentrations of TOC, respectively.

2.5. Statistical Analysis of the Results

For the statistical analysis of the results, Excel and Statistica programs were used. An analysis of variance and multiple

range test of Duncan were performed to compare the differences between evaluated samples. In all cases, 95% coverage was used. Most of the results were replicated three times and the standard deviation was reported to estimate the confidence interval.

3. Results and Discussions

3.1. Crystalline Structure and Composition

The TiO_2 is compose of anatase and brookite phases fundamentally, as it can be seen in the XRD pattern (Figure 1), where the peak 121 (characteristic of brookite) is remarkable, and the peak 110 (characteristic of rutile) is absent. The anatase 101 peak and the brookite 120 and 111 appear so near that it is not possible to distinguish between them. Despite this, the intensity ratio of brookite 111, 121 and 120 peaks is not maintained in the analyzed sample, suggesting the presence of anatase, and brookite in a lesser amount.

The broad nature peak of TiO_2 is an indication of the small crystallite size. The estimated crystallite size of TiO_2 was about 3.7 nm. Besides, no extra phases are detected, confirming the high purity of the obtained product.

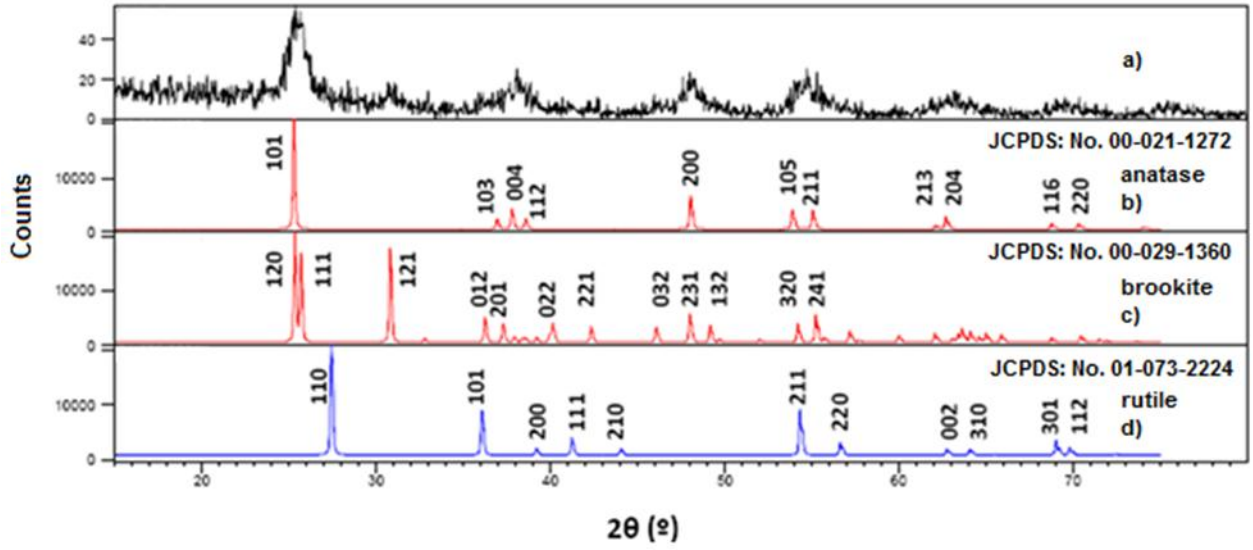

Figure 1. XRD Pattern of Synthesized TiO_2 Nanoparticles
(a) XRD Patterns of Different TiO_2 Crystalline Phases: Anatase (b), Brookite (c), Rutile (d).

Figure 2 shows the IR spectrum of the nanomaterial. Two peaks, resulting from the adsorbed water, can be observed at about 3500 cm^{-1}: stretching vibration of OH (ν_{O-H}), and at about 1600 cm^{-1}: flexing vibration peak (δ_{O-H-O}). The $\delta_{Ti-O-Ti}$ and ν_{Ti-O} peaks appear at about 500 cm^{-1} and 600 cm^{-1}, respectively [25].

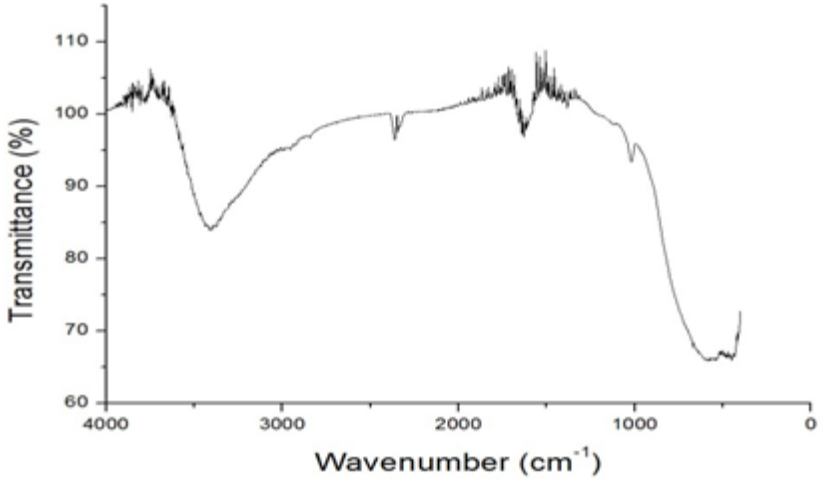

Figure 2. FT-IR Spectra of TiO_2 Nanoparticles

The composition was verified from the TEM-EDS measurements, resulting in a Ti:O molar ratio of 1:2 approximately, thus confirming that the obtained product was TiO_2. An illustrative EDS spectrum of the TiO_2 NPs is portrayed in Figure 3. Some impurities, as Cu, are present in a no significant amount.

3.2. Morphology and Surface Area

An illustrative TEM micrograph of the TiO_2 NPs is depicted in Figure 4. Some of the NPs are almost spherical, whereas others are faceted and more elongated. The TEM image indicates particle size of 9.3 nm ± 2.7 nm. TEM image (Figure 4b) shows well defined lattice fringes with a d-spacing of ~ 2.8 Å and ~ 3.5 Å, corresponding to the lattice planes (121 and 101, respectively) of the brookite and anatase TiO_2 crystal structure, respectively.

The surface area calculated according to the BET model was 115.4 m^2/g. This high value is a consequence of the small particle size of the synthesized nanomaterial.

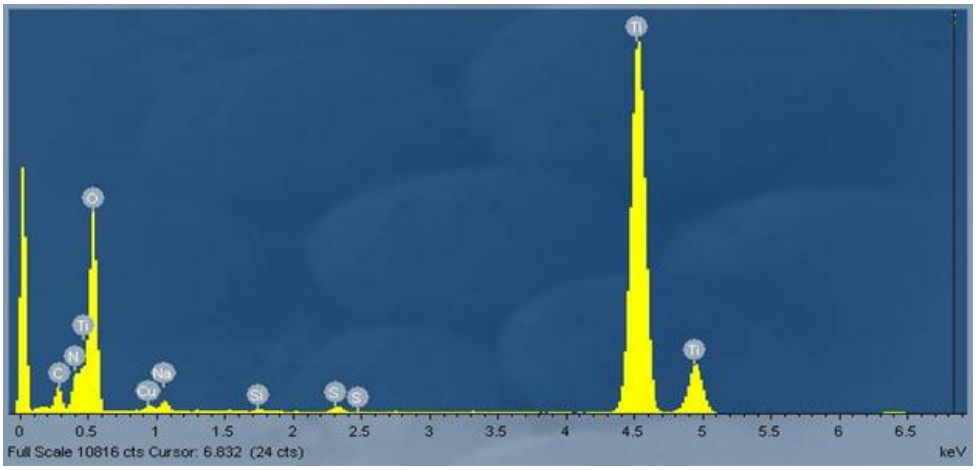

Figure 3. EDS Spectrum of TiO_2 Nanoparticles

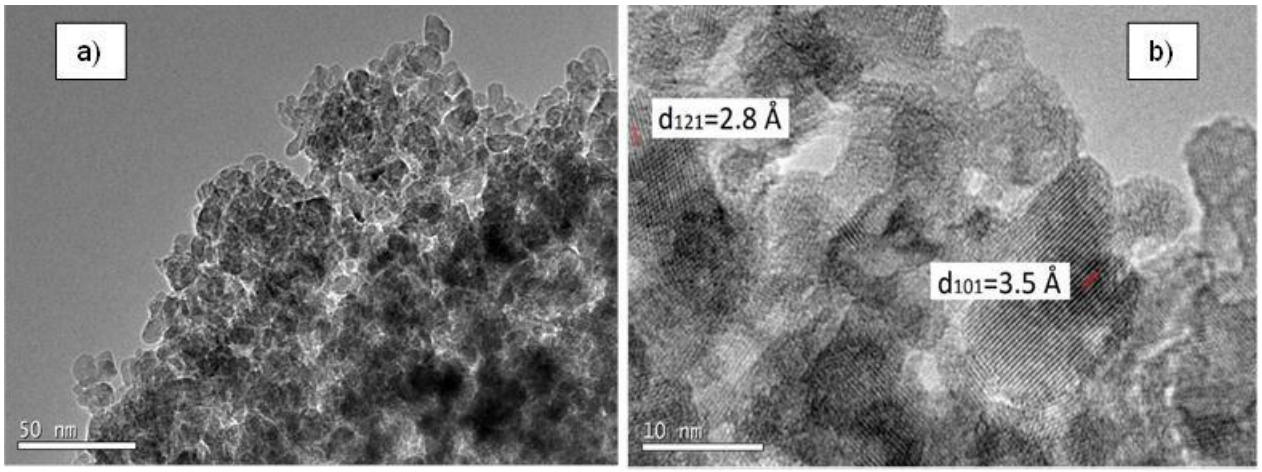

Figure 4. TEM Images of the Synthesized TiO_2 Nanoparticles
The Parallel Red Lines in b) Show a d-spacing of 2.8 Å for the Lattice Plane 121 and 3.5 Å for the Lattice Plane 101

3.3. Optical Band Gap

The transformed reflectance spectra as a function of the photon energy are depicted in Figure 5. The resulting optical band gap of the sample was found to be equal to 3.15 eV (393 nm), which is lesser that the expected *Eg* range of anatase (3.20 eV–4.50 eV) and indicates the material absorption property in the visible region (λ> 387 nm) [26].

3.4. Final Considerations about the Synthesis and Characterization

Karmaoui *et al.* [23] synthesized nanostructured TiO_2 by a solvothermal procedure, using $Ti[OC(CH_3)_3]_4$ as precursor and benzyl alcohol ($C_6H_5CH_2OH$) as solvent. The process was conducted at 180^0C for 24 h, and the product was washed with ethanol and dichloromethane and dried in air at 60^0C. This synthesis pathway generates several persistent organic compounds, where the benzyl alcohol is the most relevant because of its aromatic structure. Besides, an organometallic

precursor is used, which makes the synthesis more expensive.

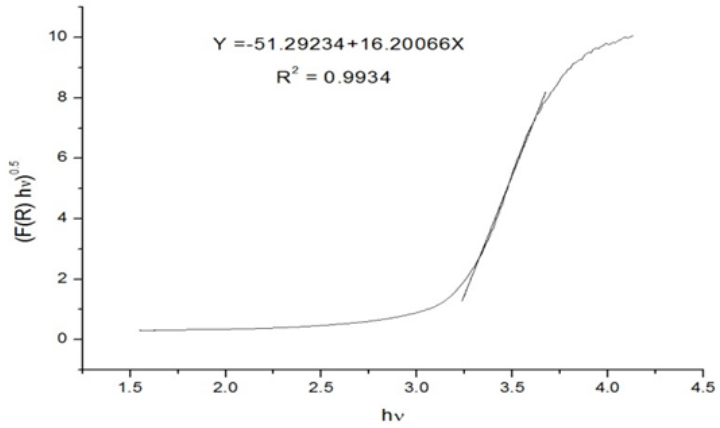

Figure 5. Kubelka–Munk Elaboration versus Energy for TiO_2 Powder

In the present work, an inexpensive residual alloy of Ti was used and it was demonstrated that there are no impurities in the final TiO_2. The surface area of the obtained TiO_2, here, was higher than Karmaoui's product (115 m^2/g vs. 95 m^2/g). Also, by the electrolytic procedure, the TiO_2 bang gap was lesser than by solvothermal procedure (393 nm vs. 385 nm), therefore our product is more sensitive to the visible spectrum. These results could be explained by the phase composition of both materials. A mixture of anatase/brookite phases was obtained by electrolysis, while only anatase was obtained by the solvothermal procedure. Different experimental studies have confirmed better photocatalytic efficiency with materials constituted by both phases (anatase and brookite) [27]. Besides, the brookite phase is more difficult to synthesize, in consequence, it has been less studied [28].

The analyzed properties are very important in order to evaluate the use of the obtained TiO_2 as photocatalyst for the degradation of POPs.

3.5. Photocatalytic Degradation of Paracetamol

The heterogeneous photocatalysis mechanism involves the participation of water and OH^- groups, adsorbed on the surface of the catalyst. The nanomaterial absorbs a light quantum and the photogenerated holes migrate to the interface and react with the OH^- groups and water to create OH radicals that can degrade the organic compounds (see Equations 5, 6 and 7) [29, 30].

$$TiO_2 + h\nu = TiO_2(h^+_{VB} + e^-_{CB}) \quad (5)$$

$$TiO_2(\mathrm{h}^+) + H_2O_{ads} = TiO_2 + OH^{\cdot}_{ads} + H^+ \quad (6)$$

$$TiO_2(\mathrm{h}^+) + OH^-_{ads} = TiO_2 + OH^{\cdot}_{ads} \quad (7)$$

Figure 6 shows the results of degradation and mineralization of paracetamol in aqueous solution with UV light, sunlight, H_2O_2 and TiO_2. Under artificial UV light exposure, the prepared titania shows photocatalytic activity exceeding in about three times (TiO_2/UV in Figure 6) the degradation with UV light alone (UV in Figure 6). However, in both cases, the degradation at 90 minutes is less than 10 %.

On the other hand, it is considerable the improvement of the photocatalytic degradation and mineralization with the addition of H_2O_2 (TiO_2/UV/H_2O_2 in Figure 6), reaching about 76 % of degradation and about 26 % of mineralization. The addition of H_2O_2 inhibits the recombination of the electron-hole pair by reacting with the excited electrons according to Equation 8, and increases the amount of generated radicals too (Equation 8). A synergic effect of paracetamol photodegradation in the presence of TiO_2 and H_2O_2 is observed if compare with the paracetamol H_2O_2 oxidation (H_2O_2 in Figure 6) and photolysis with H_2O_2 (UV/H_2O_2 in Figure 6).

$$TiO_2(\mathrm{e}^-) + H_2O_{2ads} = TiO_2 + OH^{\cdot}_{ads} + OH^- \quad (8)$$

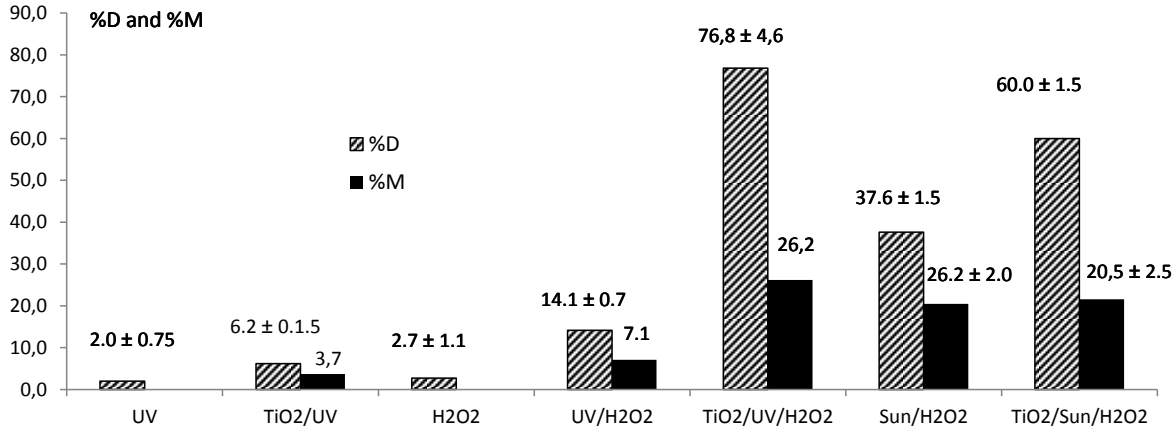

Figure 6. Degradation (%D) and mineralization (%M) of paracetamol in aqueous solution
UV: photolysis under artificial UV light. TiO_2/UV: heterogeneous photocatalysis with TiO_2 nanopowder under artificial UV light. H_2O_2: oxidation with H_2O_2. UV/H_2O_2: photolysis with H_2O_2 under artificial UV light. TiO_2/UV/H_2O_2: heterogeneous photocatalysis with TiO_2 nanopowder under artificial UV light and H_2O_2. Sun/H_2O_2: photolysis with H_2O_2 under solar radiation. TiO_2/Sun/H_2O_2: heterogeneous photocatalysis with TiO_2 nanopowder under solar radiation and H_2O_2

Moreover, the synthesized TiO_2 showed photocatalytic activity with sunlight. Degradation by heterogeneous photocatalysis (TiO_2/Sun/H_2O_2 in Figure 6) increases approximately up to 60%, comparing with degradation achieved with sunlight and peroxide alone (Sun/H_2O_2 in Figure 6). However, the mineralization stayed invariant, in these last two cases, in spite of the addition of the TiO_2.

González-Labrada [3] obtained about 30% of paracetamol degradation at equal initial concentration of the drug and pH, during 60 minutes of reaction, with commercial TiO_2 (PC 500). That result is better than the value obtained in this work, where only 6.2% of degradation was achieved. It could be explained by the differences of experimental conditions in both studies. The highest value reached by González-Labrada was obtained with a UV lamp of 24 W (more than twice the power of the lamp used in this work) and a most suitable reactor geometry (irradiation in multiple directions, because of the lamp was within the reactor), while in this work, the irradiation was unidirectional from above. Furthermore, González-Labrada bubbled dioxygen, which increases the photocatalytic activity [14].

On the other hand, Muruganandham and Swaminathan [31] studied the sunlight degradation of RO4 dye (azo compound). They used eight times the amount of TiO_2 (Degussa P25) used in this work, about 0.4 g/L of dye, 20 mmol/L of H_2O_2, pH equal to 4.8, and a steady stream of O_2, and obtained about 85% of discoloration in 20 minutes of reaction. While dyes are more sensitive to degradation by sunlight, when comparing the experimental conditions and the results obtained in this work with sunlight, it is evident the importance of adjusting experimental parameters as the mass concentration of nanomaterial, oxidizing agent (H_2O_2) and pH, in order to achieve more effective degradation.

4. Conclusions

TiO_2 nanoparticles in brookite and anatase phases were obtained by a novel synthesis method, which involves the electrolysis of a plate of Ti alloy. This method is characterized by the use of non-toxic and inexpensive reagents. The synthesized nanomaterial shows photocatalytic activity in the degradation of paracetamol in aqueous solution, which was intensified by the addition of H_2O_2. Besides, the degradation of the pollutant was achieved with sunlight, a renewable source of energy.

ACKNOWLEDGEMENTS

The authors thank Dr Luis Carlos Otero Diaz from the Department of Inorganic Chemistry, Faculty of Chemistry at University of Castilla la Mancha, Spain, for their support in the characterization of the material. Likewise the financing of TATARCOP project from InSTEC is appreciated.

REFERENCES

[1] Goi A., 2005. Advanced oxidation processes for water purification and soil remediation. Thesis to reach the degree of Doctor of Philosophy in Engineering. Tallinn, Republic of Estonia Tallinn University of Technology.

[2] Clemente A.R., Arrieta E.L.C., Mesa G.A.P., 2013. Procesos de tratamiento de aguas residuales para la eliminación de contaminantes orgánicos emergentes. Ambiente & Agua- Interdiscipl. J. Appl. Sci., 8 (3), 93-103.

[3] González-Labrada K., 2013. Sonólisis y fotólisis de paracetamol en aguas residuales. Thesis to reach the degree of Máster en Ingeniería Ambiental. La Habana, Cuba, Instituto Superior Politécnico José Antonio Echeverría (CUJAE).

[4] Cruz-González G., González-Labrada K., Milian-Rodríguez Y., Quesada-Peñate I., Colín-Luna J.A., Ramírez-Muñoz J., Jauregui-Haza U. J., 2015. Enhancement of paracetamol degradation by sono-Fenton process. Int. J. Chem. Mat. Environ. Res., 2 (4), 37-45.

[5] Espejo A., Aguinaco A., Amat A.M., Beltrán F. J., 2014. Some ozone advanced oxidation processes to improve the biological removal of selected pharmaceutical contaminants from urban wastewater. J. Environ. Sci. Health., 49 (4), 410-421.

[6] Kummerer K., 2004. Resistance in the environment. J. Antimicrob. Chemother., 54, 311-320.

[7] Yanga L., Yua L.E., Ray M. B., 2008. Degradation of paracetamol in aqueous solutions by TiO_2 photocatalysis. Water Res., 42, 3480-3488.

[8] Quesada-Peñate I., Jáuregui-Haza U., Wilhelm A. M., Delmas H., 2009. Contaminación de las aguas con productos farmacéuticos. Estrategias para enfrentar la problemática. Revista CENIC Ciencias Biológicas, 40 (3), 173-179.

[9] Graham D.W., Olivares S., Knapp C.W., Lima L., Werener D., Bowen E., 2011. Antibiotic resistance gene abundances associated with waste discharges to the Almendares river near Havana, Cuba. Environ. Sci. Technol., 45 (2),: 418-424.

[10] Keen O.S. , Linden K.G., 2013. Degradation of antibiotic activity during UV/H_2O_2 advanced oxidation and photolysis in wastewater effluent. Environ. Sci. Technol., 47, 13020-13030.

[11] Novo A., Andre S., Viana P., Nunes O.C., Manaia C.M., 2013. Antibiotic resistance, antimicrobial residues and bacterial community composition in urban wastewater. Water Res., 47, 1875-1887.

[12] Arslan I., Balcioglu I.A., Tuhkanen T., 1999. Advanced oxidation of synthetic dyehouse effluent by O_3, H_2O_2/O_3 and H_2O_2/UV processes. Environ. Technol. 20 (9), 921-931.

[13] Mahamuni N.N., Adewuyi Y.G., 2010. Advanced oxidation processes (AOPs) involving ultrasound for waste water treatment: A review with emphasis on cost estimation. Ultrason. Sonochem., 17, 990-1003.

[14] Torres-Palma R.A., Nieto J.I., Combet E., Pétrier C., Pulgarin C., 2010. An innovative ultrasound, Fe^{2+} and TiO_2 photoassisted process for bisphenol mineralization. Water Res., 44, 2245-2252.

[15] Andreozzi R., Caprio V., Insola A., Marotta R., 1999. Advanced oxidation processes (AOP) for water purification and recovery. Catal. Today. 53, 51-59.

[16] Glaze W.H., Kang J.W., Chapin D.H., 1987. The chemistry of water treatment processes involving ozone, hydrogen peroxide and UV-radiation. Ozone Sci. Eng., 9(4), 335-352.

[17] Kanakaraju D., Glass B.D., Oelgemöller M., 2014. Titanium dioxide photocatalysis for pharmaceutical wastewater treatment. Environ. Chem. Lett., 12, 27-47.

[18] Muir N., Nichols J.D., Clifford J. M., Sykes J., 1997. Comparative bioavailability of aspirin and acetaminophen following single dose administration of solution and plain tables. Current Med. Res. Opinion., 13, 491-500.

[19] Bedner M., Maccrehan W., 2006. Transformation of acetaminophen by chlorination produces the toxicants 1,4- benzoquinone and N-acetyl-p-benzoquinone imine. Environ. Sci. Technol., 40, 516-522.

[20] Peláez E., Müller W.D., Ruiz A., Valdés M., Fernández D., 2012. Procedimiento para la síntesis electrolítica de polvo nanométrico y nanoestructurado de óxido de titanio (IV). Oficina Cubana de la Propiedad Industrial, No. 2012-0104.

[21] Ruiz A., 2010. Síntesis electroquímica y caracterización del polvo nanométrico de TiO_2. Thesis to reach the degree of Licenciado en Química. La Habana, Cuba, Universidad de la Habana.

[22] Marfunin A., 1979. Physics of minerals and inorganic materials: an introduction: Springer-Verlag.

[23] Karmaoui M., Tobaldi D.M., Skapin A.S., Pullar R.C., Seabra M.P., Labrincha J.A., Amaral V.S., 2014. Non-aqueous sol–gel synthesis through a lowtemperature solvothermal process of anatase showing visible-light photocatalytic activity. RSC Adv. 4, 46762–46770.

[24] Will I.B.S., Moraes J.E.F., Teixeira A.C.S.C., Guardani R., Nascimento C.A.O., 2004. Photo-Fenton degradation of wastewater containing organic compounds in solar reactors. Sep. Purif. Technol., 34, 51–57.

[25] Lin J., Lin Y., Liu P., Meziani M., Allard L., Sun Y., 2002. Hot-fluid annealing for crystalline titanium dioxide nanoparticles in stable suspension. J. Am. Chem. Soc., 124 (38), 115-148.

[26] Wang J., Zhao G., Zhang Z., Zhang X., Zhang G., Ma T., Li Y. , ., 2007. Investigation on degradation of azo fuchsine using visible light in the presence of heat-treated anatase TiO_2 powder. Dyes Pigments., 75, 335-343.

[27] Paola A.D., Bellardita M., Palmisano L., 2013. Brookite, the least known TiO_2 photocatalyst. Catal., 3, 36-73.

[28] Hanaor D.A.H., Sorrell C.C., 2011. Review of the anatase to rutile phase transformation. J. Mater. Sci., 46, 855–874.

[29] Kontos A.I., Arabatzis I.M., Tsoukleris D.S., Kontos A.G., Bernard M.C., Petrakis D.E., Falaras P., 2005. Efficient photocatalysts by hydrothermal treatment of TiO_2. Catal. Today, 101, 275-281.

[30] Rajeshwar K., Osugi M.E., Chanmanee W., Chenthamarakshan C.R., Zanoni M.V.B., Kajitvichyanukul P., Krishnan-Ayer R., 2008. Heterogeneous photocatalytic treatment of organic dyes in air and aqueous media. J. Photochem. Photobiol., C: Photochem. Rev., 9, 171-192.

[31] Muruganandham M., Swaminathan M., 2004. Solar photocatalytic degradation of a reactive azo dye in TiO_2-suspension. Sol. Energy Mater. Sol. Cells, 81, 439-457.